INFECTION AND IMMUNITY, Apr. 2011, p. 1536–1545 Vol. 79, No. 4
0019-9567/11/$12.00 doi:10.1128/IAI.01104-10

Antibiotic Treatment Alters the Colonic Mucus Layer and Predisposes the Host to Exacerbated *Citrobacter rodentium*-Induced Colitis▽

M. Wlodarska,[1,2] B. Willing,[1] K. M. Keeney,[1] A. Menendez,[1] K. S. Bergstrom,[3] N. Gill,[1] S. L. Russell,[1,2] B. A. Vallance,[3] and B. B. Finlay[1,2,4]*

Michael Smith Laboratories, University of British Columbia, Vancouver, British Columbia, Canada V6T 1Z4[1]; Department of Microbiology and Immunology, University of British Columbia, Vancouver, British Columbia, Canada V6T 1Z4[2]; Department of Pediatrics, Division of Gastroenterology, Child and Family Research Institute, Vancouver, British Columbia, Canada V5Z 4H4[3]; and Department of Biochemistry and Molecular Biology, University of British Columbia, Vancouver, British Columbia, Canada V6T 1Z4[4]

Received 15 October 2010/Returned for modification 15 November 2010/Accepted 2 February 2011

Antibiotics are often used in the clinic to treat bacterial infections, but the effects of these drugs on microbiota composition and on intestinal immunity are poorly understood. *Citrobacter rodentium* was used as a model enteric pathogen to investigate the effect of microbial perturbation on intestinal barriers and susceptibility to colitis. Streptomycin and metronidazole were used to induce alterations in the composition of the microbiota prior to infection with *C. rodentium*. Metronidazole pretreatment increased susceptibility to *C. rodentium*-induced colitis over that of untreated and streptomycin-pretreated mice, 6 days postinfection. Both antibiotic treatments altered microbial composition, without affecting total numbers, but metronidazole treatment resulted in a more dramatic change, including a reduced population of *Porphyromonadaceae* and increased numbers of lactobacilli. Disruption of the microbiota with metronidazole, but not streptomycin treatment, resulted in an increased inflammatory tone of the intestine characterized by increased bacterial stimulation of the epithelium, altered goblet cell function, and thinning of the inner mucus layer, suggesting a weakened mucosal barrier. This reduction in mucus thickness correlates with increased attachment of *C. rodentium* to the intestinal epithelium, contributing to the exacerbated severity of *C. rodentium*-induced colitis in metronidazole-pretreated mice. These results suggest that antibiotic perturbation of the microbiota can disrupt intestinal homeostasis and the integrity of intestinal defenses, which protect against invading pathogens and intestinal inflammation.

The intestinal microbiota can be thought of as an organ system, essential for nutrient acquisition, metabolism of indigestible compounds, defense against colonization by pathogens, and the development of intestinal architecture and the immune system (40, 43). Compositional changes in the intestinal microbiota can lead to severe dysregulation of the physiological and immunological intestinal homeostasis, with serious adverse consequences for the host (43). A well-known case of this is antibiotic treatment, and previous studies have shown that antibiotic treatment can predispose the host to enteric infections (48). A recent investigation by Sekirov et al. showed that various doses of antibiotic treatments predispose mice to increased colonization by *Salmonella enterica* serovar Typhimurium and intestinal pathology (48). Additionally, Brandl et al. showed that administration of a broad-spectrum combination of metronidazole (Met), neomycin, and vancomycin promotes infection by vancomycin-resistant enterococci (9). Further, there are significant differences in microbiota compositions of inflammatory bowel disease (IBD) patients and healthy individuals, further implicating microbial factors in the initiation and perpetuation of colitis (17, 19, 32, 46). It is unknown if such changes precede and contribute to the onset of IBD or are simply a result of IBD. Moreover, antibiotics are used extensively with variable efficacy in the treatment of IBDs, such as ulcerative colitis (20, 45). As the molecular basis of the microbiota's protective effects and the processes triggered as a result of its perturbation are not fully understood, it is important to elucidate the mechanisms by which antibiotic-induced microbial shifts perturb the homeostatic state of the intestinal immune system. While the microbiota likely represent a physical barrier that prevents pathogens from interacting with and penetrating the intestinal mucosa (50), other studies suggest a much higher degree of complexity that involves a direct role for the microbiota in dictating the immunological tone of the intestine (12, 24, 44).

The intestinal epithelium and its protective mucin cover are the primary defenses against pathogen permeation and microbial leakage into the underlying lamina propria (LP). Antimicrobial proteins secreted by intestinal epithelial cells (IECs) include defensins, cathelicidins, and C-type lectins (Reg3β and Reg3γ) (23). They function by disrupting bacterial surface structures and contribute to the maintenance of microbiota composition. Their expression has been shown to rely on IEC stimulation by microbes and their products (12). Additionally, recognition of commensals by IECs has been shown to be important in regulating the inflammatory state of the intestine, through regulation of the interleukin-25 (IL-25)–IL-23–IL-17 axis and Th17 cells (59).

Goblet cells, a type of specialized IECs, have a protective role in the intestine through the production of bioactive com-

* Corresponding author. Mailing address: #301-1285 East Mall, Michael Smith Building, University of British Columbia, Vancouver, BC V6T 1Z4, Canada. Phone: (604) 822-2210. Fax: (604) 822-9830. E-mail: bfinlay@interchange.ubc.ca.

▽ Published ahead of print on 14 February 2011.

pounds, including mucins, trefoil factors, and other antimicrobials (53, 56). These molecules provide defense against pathogens by preventing bacterial penetration of the intestinal epithelium, and they play a key role in the maintenance of healthy intestinal homeostasis (35). Studies using mucin-knockout mice, germfree (GF) mice, and probiotics suggest that the intestinal mucus layer is a major mediator of microbe-IEC interactions and that mucus integrity is largely affected by the microbiota (26, 34, 55). The mucus layer in the large intestine consists of two stratified layers mainly composed of the secreted mucin Muc2 (26). The inner mucus layer composition is dense and devoid of the microbiota, while the outer layer is a loose matrix that houses the microbiota (26). The inner dense mucus layer functions as a barrier, which serves to minimize microbial translocation and prevent excessive immune activation (22). Mice deficient in Muc2 production have an altered intestinal mucus layer and spontaneously develop colitis, suggesting that defects in mucin production lead to altered microbe-IEC interactions (55). Microbes might interact with IECs by diffusion of microbe-associated molecular patterns (MAMPs) through the mucus layer, resulting in stimulation of the underlying IECs (23). Under homeostatic conditions, this bacterial stimulation comes from the microbiota and seems to be important for a healthy mucus layer, as GF mice produce an inner mucus layer that is thinner than that of conventionally housed mice (26).

This study aimed to define the effect of metronidazole (Met) and streptomycin (Strep) on mucosal defense. We hypothesized that an alteration in intestinal microbial composition by antibiotic treatments would alter susceptibility to the natural mouse pathogen *Citrobacter rodentium*, which results in intestinal inflammation with features similar to those of ulcerative colitis (38). Both antibiotics induced distinct alterations in the microbiota composition, altering the susceptibility of the host to subsequent *C. rodentium*-induced colitis. We found that mice pretreated with metronidazole suffer a more severe form of *C. rodentium*-induced colitis than do streptomycin-pretreated and untreated mice. Further, our results demonstrate that some antibiotic treatments can not only induce compositional changes in the commensal population but also affect the inflammatory tone of the intestine, interfering with the protective function of goblet cells. Metronidazole treatment reduced Muc2 production and caused a thinning of the protective mucus layer, suggesting that intestinal homeostatic changes and depletion of the mucus layer by some antibiotics may predispose the host to enteric infection and, potentially, other inflammatory bowel diseases.

MATERIALS AND METHODS

Mice. Eight- to 10-week-old C57BL/6 female mice (Jackson Laboratory, Bar Harbor, ME) were housed in the animal facility at the University of British Columbia (UBC) in accordance with guidelines of the UBC Animal Care Committee and the Canadian Council on the Use of Laboratory Animals. Mice were fed a standard sterile chow diet (laboratory rodent diet 5001; Purina Mills, St. Louis, MO) *ad libitum* throughout the experiments. Antibiotic-treated mice were given metronidazole (Sigma) at 750 mg/liter or streptomycin (Sigma) at 450 mg/liter in drinking water for 4 days. Untreated, control mice received sterilized water. After 4 days, the antibiotics were withdrawn, mice were infected or euthanized, and tissues were harvested.

Bacterial strains and infection of mice. Mice were infected by oral gavage with 0.1 ml of an overnight culture of LB containing approximately 2.5×10^8 CFU of a streptomycin-resistant derivative of *C. rodentium* DBS100.

Tissue collection. Uninfected mice or mice at days 2, 4, 6, and 21 postinfection (p.i.) were euthanized by CO_2 asphyxiation, and their spleens, mesenteric lymph nodes (mLNs), and large intestines were dissected for further analysis. The large intestine was divided into cecum and colon. The piece of the distal colon collected for subsequent studies was the terminal 5 mm. Tissues were immediately placed in 10% neutral buffered formalin for histological studies or methanol-Carnoy's fixative for mucin studies or frozen at −20°C for subsequent microbial composition analysis.

Microbial composition analysis. Changes in microbial composition were assessed in tissue samples collected from the distal colon by terminal restriction fragment length polymorphism (T-RFLP) analysis and cloning and sequencing as previously described (57). Briefly, total bacterial 16S rRNA genes were PCR amplified using broad-range *Eubacteria* primers 27F and 926r (Table 1) and subjected to digestion with HaeIII and MspI. Fragment length determination of 6-carboxyfluorescein (6-FAM)-labeled products was performed on an ABI 3730 capillary sequencer (Applied Biosystems), and electropherograms were processed using GeneMarker (State College, PA). Peaks of interest were compared to reference clone libraries generated using DNA isolated from the ileum, cecum, and feces of C57BL/6 mice treated with streptomycin or metronidazole or not treated. PCR-amplified products were cloned into the pCR 4 TOPO vector and transformed into *Escherichia coli* TOP10 chemically competent cells (Invitrogen). Sequences were classified using the naïve Bayesian rRNA classifier in RDP (57). Real-time PCRs were completed using 16S rRNA group-specific primers (Table 1) to determine the relative abundances of selected bacterial groups (standard curves from ATCC strains or purified 16S rRNA gene clones) including *Bacteroidales* (purified clone), *Bifidobacterium* (purified clone), *Clostridium coccoides* cluster (ATCC 47340D), and *Lactobacillus* (ATCC 4357D) in colon samples. Results were normalized to total bacterial 16S rRNA gene copies in the sample. To test whether treatments resulted in reduced bacterial abundance, total bacterial 16S rRNA gene copies were also quantified in fecal samples, because colon samples had various contents of digesta. Measurement of 16S rRNA gene copies correlates well with bacterial number. All real-time PCRs were performed using Quantitect SYBR-Green Mastermix (Qiagen).

***Citrobacter rodentium* CFU and cytokine determination.** Whole mLNs, ceca, and colon tissues were collected in 1 ml of sterile phosphate-buffered saline (PBS) supplemented with complete EDTA-free protease inhibitor cocktail (Roche Diagnostics) at a final concentration recommended by the manufacturer. Tissues were weighed and homogenized in a MixerMill 301 bead miller (Retche) for 5 min at 30 Hz at room temperature. Tissue homogenates were serially diluted in PBS, plated onto MacConkey agar (Difco), and incubated overnight at 37°C, and bacterial colonies were enumerated the following day and normalized to the tissue weight (per gram). *C. rodentium* colonies were clearly identified by their unique characteristic of being round with a red center and a white rim. Colon homogenates were centrifuged twice at 15,000 × *g* for 20 min at 4°C to remove cell debris, and the supernatants were aliquoted and stored at −80°C. Cytokine levels in colon homogenates were determined with the BD cytometric bead array mouse inflammation kit (BD Biosciences), according to the manufacturer's recommendations, and normalized to tissue weight (per gram).

Immunohistochemistry. Sections of 5 μm were deparaffinized and rehydrated. Antigen retrieval was performed prior to blocking and staining by placing deparaffinized, rehydrated slides in 10 mM citric acid (pH 6.0) at 90 to 100°C for 20 min, followed by cooling to room temperature. Immunostaining was carried out using antibodies against Tir (antibody production described previously [14]) or murine Muc2 (H-300; Santa Cruz Biotechnology) antibody at 4°C overnight followed by incubation with an Alexa 488-conjugated secondary antibody (Invitrogen) for 1 h at room temperature. Tissues were mounted using ProLong Gold Antifade (Molecular Probes/Invitrogen) containing 4′,6-diamidino-2-phenylindole (DAPI) for DNA staining.

Fluorescence-activated cell sorting (FACS) analysis. Lamina propria cells were isolated from the excised murine colon. The colon was opened longitudinally for washing and diced in small, 0.5-cm sections. These sections were treated with collagenase from *Clostridium histolyticum* VIII (Sigma) at 37°C for 1 h. The cell suspension was purified using a 30% Percoll gradient. Purified splenic and lamina propria cells were stained with fluorochrome-conjugated antibodies against CD45, CD3e, CD49b (clone DX5), and F480 (all from BD Biosciences) before being analyzed with an LSR II flow cytometer (BD Biosciences) using CellQuest and FlowJo 6.1.1 software.

RNA isolation and cDNA synthesis. The terminal 2 to 3 mm of the colon was excised, immediately submerged in RNA*later* (Qiagen), and stored at 4°C overnight and then at −80°C for subsequent RNA extraction. RNA was extracted using the RNeasy minikit (Qiagen) according to the manufacturer's instructions. RNA concentration was determined using a NanoDrop ND-1000 spectrophotometer (NanoDrop Technologies, Wilmington, DE), and reverse transcription

TABLE 1. Sequences of primers for microbiota composition and host gene expression analysis

Target[a]	Primer	Sequence	T_a[c] (°C)
Eubacteria 16S rRNA (T-RFLP and cloning)	Bact-27f[b]	AGAGTTTGATCMTGGCTCAG	55
	926r	CCGTCAATTCCTTTRAGTTT	
Eubacteria 16S rRNA (total bacteria) (1)	UniF340	ACTCCTACGGGAGGCAGCAGT	63
	UniR514	ATTACCGCGGCTGCTGGC	
Bacteroidales 16S rRNA (16)	BactF285	GGTTCTGAGAGGAAGGTCCC	61
	UniR338	GCTGCCTCCCGTAGGAGT	
Bifidobacterium 16S rRNA (30)	Bif164F	GGGTGGTAATGCCGGATG	62
	Bif662R	CCACCGTTACACCGGGAA	
Clostridium coccoides 16S rRNA (18)	UniF338	ACTCCTACGGGAGGCAGC	60
	CcocR491	GCTTCTTAGTCAGGTACCGTCAT	
Lactobacillus 16S rRNA (42)	LabF362	AGCAGTAGGGAATCTTCCA	56
	LabR677	CACCGCTACACATGGAG	
Muc2 (21)	MUC2-F	GCTGACGAGTGGTTGGTGAATG	60
	MUC2-R	GATGAGGTGGCAGACAGGAGAC	
TFF3 (21)	TFF3-F	CCTGGTTGCTGGGTCCTCTG	60
	TFF3-R	GCCACGGTTGTTACACTGCTC	
GAPDH	GAPDH-F	ATTGTCAGCAATGCATCCTG	60
	GAPDH-R	ATGGACTGTGGTCATGAGCC	

[a] Numbers in parentheses are references.
[b] 6-FAM-labeled 5′ end for T-RFLP.
[c] T_a, annealing temperature.

(RT) was performed with the Quantitect RT kit (Qiagen) using 1 μg RNA as template.

Real-time PCR. Real-time PCR was performed using Quantitect SYBR-Green Mastermix (Qiagen) and QuantiTect Reg3γ, Relmβ, IL-25, and thymic stromal lymphopoietin (TSLP) primers (Qiagen) in addition to the primers listed in Table 1. PCR was performed on an Opticon 2 system (Bio-Rad), and cycles consisted of 95°C for 15 min and 40 cycles of 94°C for 15 s, 60°C for 30 s, and 72°C for 30 s. Glyceraldehyde-3-phosphate dehydrogenase (GAPDH) was used for normalization. The fold difference in expression was calculated as threshold cycle ($2^{-\Delta\Delta CT}$).

Measurements of mucus thickness *ex vivo*. The terminal 5 mm of the colon was excised, immediately submerged in methanol-Carnoy's fixative at 4°C for 2 h, and then placed into 100% ethanol. Fixed colon tissues were embedded in paraffin and cut into 5-μm sections. Tissues were stained with Alcian Blue (AB)/periodic acid-Schiff (PAS) stain.

Histopathological scoring. Tissues were fixed in 10% neutral buffered formalin overnight and then placed into 70% ethanol. Fixed cecal tissues were embedded in paraffin and cut into 5-μm sections. Tissues were stained with hematoxylin and eosin (H&E) using standard techniques by the UBC Histology Laboratory. Tissue sections were assessed for pathology in four regions: lumen, surface epithelium, mucosa, and submucosa. Pathology in the lumen was based on the presence of necrotic epithelial cells (0, none; 1, scant; 2, moderate; 3, dense). The surface epithelium was scored for regenerative change (0, none; 1, mild; 2, moderate; 3, severe), desquamation (0, no change; 1, <10 epithelial cells shedding per lesion; 2, 11 to 20 epithelial cells shedding per lesion), and ulceration (3, epithelial ulceration; 4, epithelial ulceration with severe crypt destruction). The mucosa was scored for hyperplasia (scored based on crypt length/high-power field averaged from four fields at ×400 magnification where 0 is <140 μm, 1 is 141 to 285 μm, 2 is 286 to 430 μm, and 3 is >431 μm) and goblet cell depletion (scored based on number of goblet cells/high-power field averaged from four fields at ×400 magnification where 0 is >50, 1 is 25 to 50, 2 is 10 to 25, and 3 is <10). Lastly, the submucosa was scored for edema (0, no change; 1, mild; 2, moderate; 3, profound). The maximum score that could result from this scoring is 21.

Statistical analysis. T-RFLP profiles were subjected to cluster analysis using Bray-Curtis metrics (31). Statistical significance was calculated by using a two-tailed Student *t* test unless otherwise stated, with assistance from GraphPad Prism software version 4.00 (GraphPad Software, San Diego, CA). If not otherwise specified, statistical significance was indicated as follows: ***, $P < 0.001$; **, $P < 0.01$; *, $P < 0.05$; NS (not significant), $P > 0.05$. The results are expressed as the mean value with standard error of the mean (SEM), unless otherwise indicated.

RESULTS

Metronidazole pretreatment increases the severity of *C. rodentium*-induced colitis. To study the role of the microbiota in protection against enteric infections, two different antibiotics, streptomycin and metronidazole, were used to induce alterations in the intestinal microbial composition prior to infection with *C. rodentium*. Streptomycin is a broad-spectrum antibiotic that kills sensitive microbes by binding to the 30S subunit of the bacterial ribosome and inhibiting protein synthesis (7). Metronidazole targets anaerobic bacteria and sensitive protozoa, as these organisms are capable of nitroreduction of metronidazole, converting it to its active form, leading to DNA damage (47). An analysis of the ceca from metronidazole-pretreated, infected mice 6 days postinfection (p.i.) showed inflammation that was significantly increased over that of untreated, infected mice (Fig. 1A to C). This was characterized by greater submucosal edema, more extensive damage to the surface mucosa and ulceration, extensive regions of mucosal hyperplasia, and increased goblet cell depletion in metronidazole-pretreated mice 6 days p.i. (Fig. 1B). At 6 days p.i., streptomycin-pretreated mice showed overall pathology not significantly different from that of untreated mice (Fig. 1C). This study focused on cecal pathology since the cecum is the first site colonized by *C. rodentium*, and as a result, it exhibits

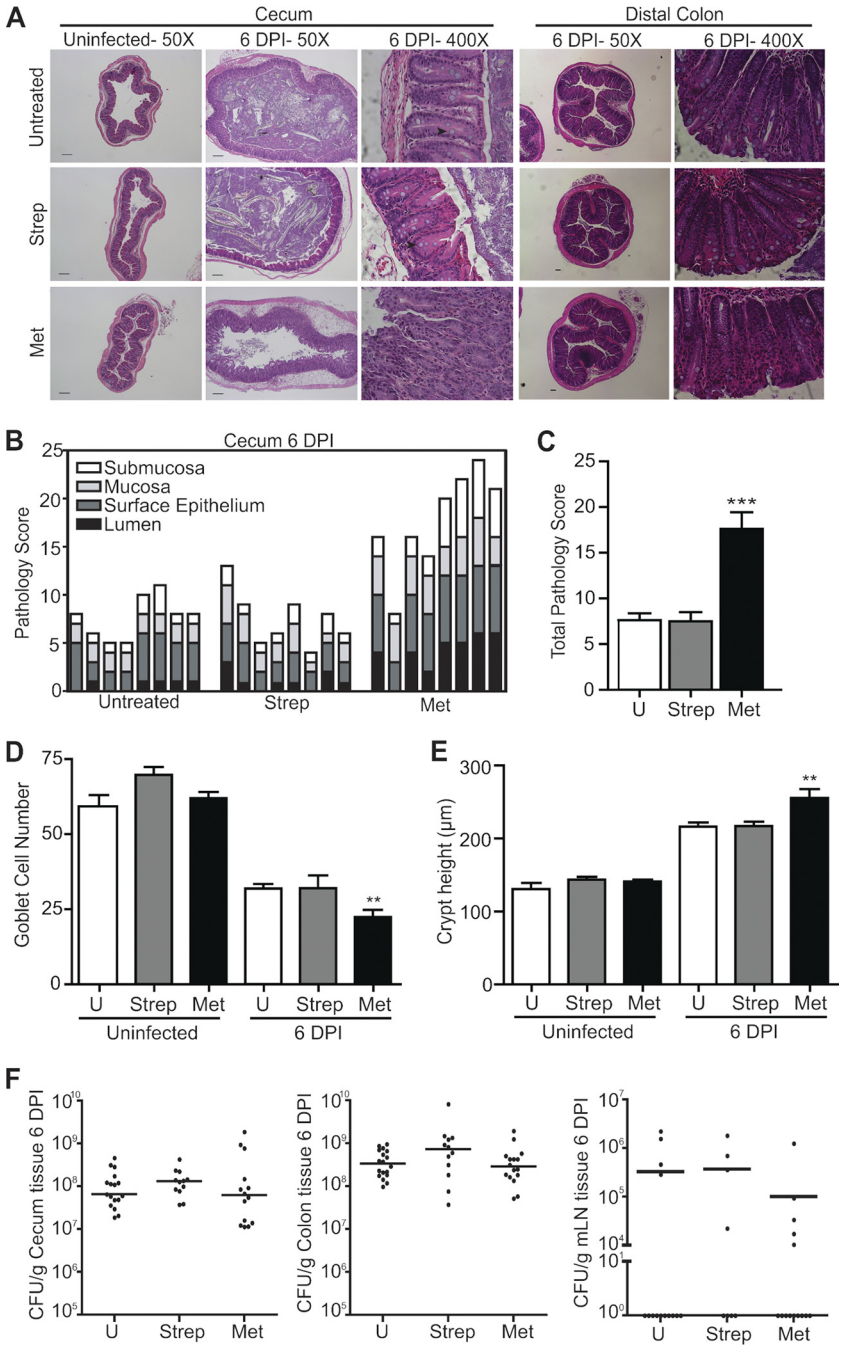

FIG. 1. Metronidazole pretreatment leads to increased severity of *C. rodentium*-induced colitis. (A) H&E-stained cecal and distal colon sections from untreated and streptomycin- and metronidazole-pretreated mice at day 0 and 6 days p.i. No inflammation is evident in cecal sections of untreated and antibiotic-pretreated mice prior to infection (left panels; original magnification, ×50; bars, 100 μm). Notably, there is an increase in inflammation throughout the cecal mucosa and submucosa of metronidazole-pretreated mice (original magnification, ×50; bars, 100 μm). Goblet cell depletion and hyperplasia are more extensive in the mucosa of metronidazole-pretreated mice (black arrowhead, goblet cell; right panels; original magnification, ×400) both in the cecum and in the distal colon. (B) Independent histology damage scores from cecal tissues of untreated, streptomycin-pretreated, and metronidazole-pretreated mice at day 6 p.i. Scores were determined under blinded conditions. Each bar represents one individual based on inflammation and damage to the submucosa, mucosa, surface epithelium, and lumen. (C) Cumulative histology damage scores from cecal tissue at day 6 p.i. of untreated, streptomycin-pretreated, and metronidazole-pretreated mice. Scores were determined under blinded conditions. Cecal results represent the means of two independent infections ($n = 4$ per group). U, untreated; ***, $P = 0.0003$. (D) Goblet cell numbers of untreated, streptomycin-pretreated, and metronidazole-pretreated mice. Goblet cell numbers prior to infection and at day 6 p.i. in the distal colon are shown. Results represent the means of two independent experiments ($n = 4$ per group). U, untreated; **, $P = 0.0011$. (E) Hyperplasia was measured as changes in crypt length in untreated, streptomycin-pretreated, and metronidazole-pretreated mice. Hyperplasia prior to infection and that at day 6 p.i. in the distal colon are shown. Results represent the means of two independent experiments ($n = 4$ per group). U, untreated; **, $P = 0.0044$. (F) Enumeration of *C. rodentium* bacteria in the cecum, colon, and mesenteric lymph node tissue at day 6 p.i. Each data point represents one individual. Results are pooled from three separate infections ($n = 4$ to 6 per group). The horizontal lines represent the median for each group. U, untreated.

inflammation and tissue pathology before the distal colon does. However, we did note that metronidazole treatment results in a modest increase in distal colon pathology 6 days p.i., with significantly greater goblet cell depletion and hyperplasia (Fig. 1D and E). Later in the infection, 10 days p.i., there is increased pathology in the distal colon of metronidazole-pretreated mice compared to that in streptomycin-treated and untreated mice (data not shown). Increased mucosal damage seen in metronidazole-pretreated, infected mice was not due to increased *C. rodentium* burdens, as numbers were similar to those in untreated and streptomycin-pretreated mice in the cecum, colon, and mesenteric lymph nodes, 6 days p.i. (Fig. 1F).

In order to elucidate any competitive advantage given to *C. rodentium* specific to metronidazole pretreatment, and not to streptomycin pretreatment, we determined total microbial numbers and composition in the large intestine prior to infection. Total fecal microbial numbers, as determined by real-time PCR, were not significantly affected by either 4-day antibiotic treatment (Fig. 2A). Conversely, both streptomycin and metronidazole had distinct effects on the bacterial community composition of the distal colon, as assessed by terminal restriction fragment length polymorphism (T-RFLP) (Fig. 2B). Terminal restriction fragment lengths that differed between treatments were compared to established clone libraries and validated by quantitative PCR (qPCR). Streptomycin treatment resulted in substantial changes to the microbiota composition; however, it did not affect the abundance of the *Bacteroidales* order, specifically the *Porphyromonadaceae* family (Fig. 2B). *Porphyromonadaceae* represent the most abundant family of the *Bacteroidales* order found in untreated mice. Metronidazole treatment resulted in a more significant disturbance in the microbial composition of the colon than did streptomycin treatment (Fig. 2B). Metronidazole depleted the population of obligate anaerobic *Bacteroidales*, but aerotolerant populations, including lactobacilli, became more abundant, resulting in no significant effect of metronidazole on total bacterial numbers (Fig. 2A and C). Conversely, streptomycin depleted the lactobacillus population (Fig. 2C). The *Clostridium coccoides* group was also depleted by metronidazole treatment, while streptomycin resulted in partial depletion, although not significant, compared to the control (Fig. 2C). *Bifidobacterium* spp., which were previously correlated with increased mucus thickness (41), were undetected in all treatment groups. The differential shift in microbial composition between streptomycin- and metronidazole-treated mice confirms the distinct effect of either antibiotic on the host microbiota.

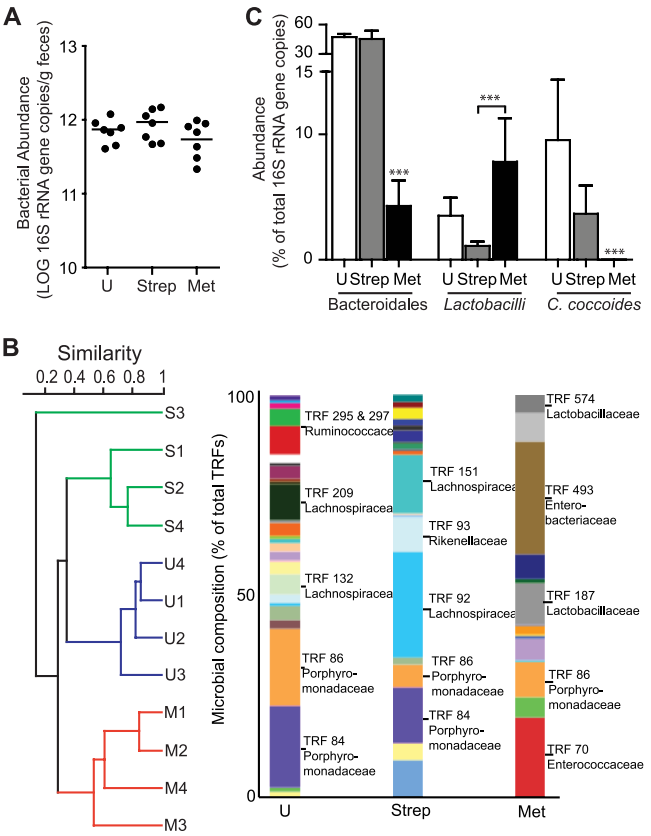

FIG. 2. Metronidazole treatment and streptomycin treatment of mice differentially alter the microbial composition of the colon compared to that of untreated mice. (A) Total bacterial numbers determined by real-time PCR measuring *Eubacteria* 16S rRNA in feces of untreated (U) and streptomycin- and metronidazole-treated mice. Results are averaged from two independent experiments ($n = 3$ or 4 mice per group). (B) Similarity tree using Bray-Curtis metrics of bacterial 16S rRNA gene terminal restriction fragment profiles from distal colon samples. Bar graphs represent average T-RFLP profiles from each treatment group, and the bacterial families represented by terminal restriction fragment lengths (TRFs; cut with MspI) of interest are indicated. U, untreated mice; S, streptomycin-treated mice; M, metronidazole-treated mice. Results are representative of two independent experiments ($n = 3$ or 4 mice per group). (C) Real-time PCR quantification of select bacterial populations using group-specific primers on DNA extracted from distal colon samples. The abundance of target groups was normalized to the total bacterial 16S rRNA gene copies in each sample. Results are averaged from two independent experiments ($n = 3$ or 4 mice per group). ***, $P < 0.0001$.

Metronidazole treatment increases the inflammatory tone of the colon. To understand the mechanism underlying the increased *C. rodentium*-induced damage observed in metronidazole-treated mice, we analyzed the effect of the antibiotic treatments on several parameters of intestinal immune function. As shown in Fig. 3A, a 4-day treatment with either antibiotic did not result in overt intestinal inflammation. However, metronidazole-treated mice, but not streptomycin-treated mice, showed an increase in mRNA expression of both *IL-25* and *Reg3*γ, but not *thymic stromal lymphopoietin* (*TSLP*), indicating increased microbial stimulation of the intestinal epithelium (Fig. 3B) (12, 59). The spleen and colon of untreated and metronidazole-treated mice were excised, and cells were isolated for FACS analysis. Increased stimulation of the epithelium after metronidazole treatment had no effect on colonic T cell numbers (Fig. 3C) but resulted in increased macrophage and NK cell infiltration of the intestinal lamina propria (LP); metronidazole-treated mice exhibited a 3-fold increase in the frequency of macrophages ($P = 0.0382$) and a 4-fold increase in the frequency of NK cells ($P = 0.0225$) (Fig. 3C and E). In contrast, splenic NK and macrophage cell numbers were unchanged by metronidazole treatment (Fig. 3D and E), indicating that the increased frequency of these innate immune cells is a local (intestinal) and not a systemic effect of metronidazole.

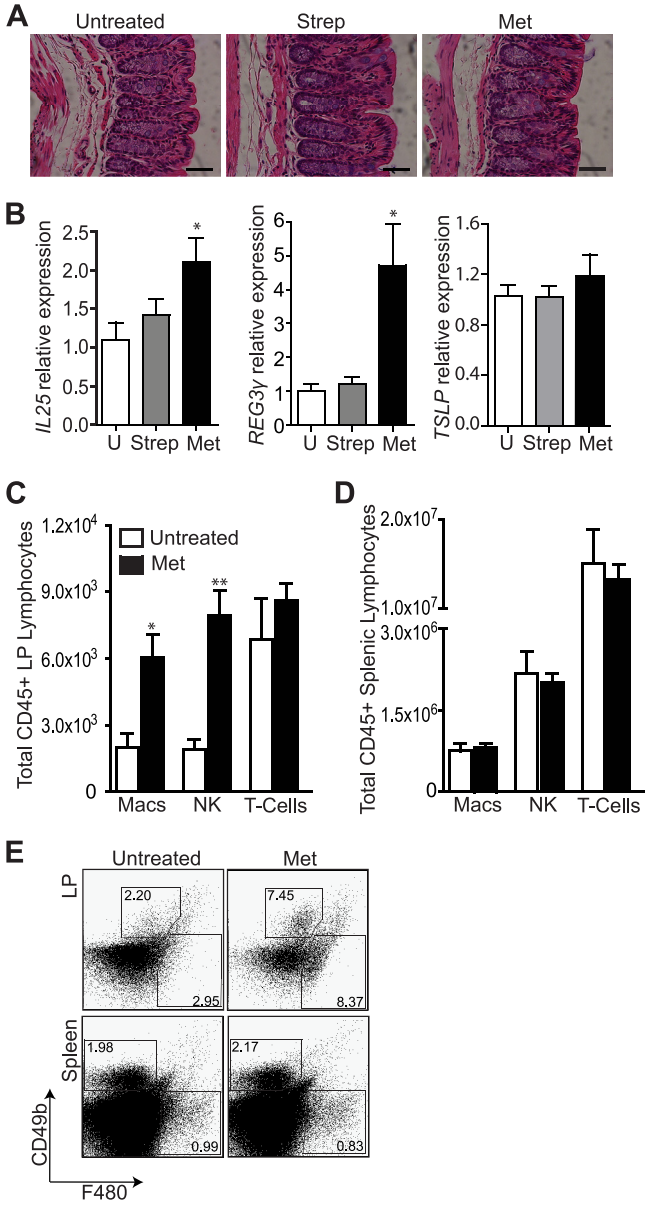

FIG. 3. Metronidazole treatment alters the homeostatic balance of the distal colon. (A) H&E-stained distal colon sections from untreated and streptomycin- and metronidazole-treated mice at day 0. No overt inflammation evident. Original magnification, ×400; bars, 50 μm. (B) Quantitative RT-PCR results of *IL-25* (*, $P = 0.0371$), *Reg3*γ (*, $P = 0.0177$); and *TSLP* expression in the distal colon of untreated and streptomycin- and metronidazole-treated mice. Results are averaged from three independent experiments ($n = 4$ to 6 mice per group). U, untreated mice. (C and D) FACS analysis of macrophage, NK cell, and T cell recruitment to the lamina propria (C) and spleen (D) in untreated and metronidazole-treated mice. Both splenic and lamina propria cells were stained with fluorescently labeled CD45, CD3ε, CD49b, and F480. Only CD45-positive cells were examined for the expression of CD3ε, CD49b, and F480. T cells are defined as $CD45^+$ $CD3\varepsilon^+$ $CD49b^-$; NK cells are defined as $CD45^+$ $CD3\varepsilon^-$ $CD49b^+$; macrophages are defined as $CD45^+$ $F480^+$. (E) Flow cytometric analysis of $CD49b^+$ and $F480^+$ populations within the $CD45^+$ lymphocytes in the lamina propria and spleen of untreated and metronidazole-treated mice. Data from one mouse per group are shown and are representative of 2 independent experiments ($n = 4$ per group).

Metronidazole treatment compromises goblet cell function and inner mucus layer production. Metronidazole-treated animals showed evidence of increased bacterial stimulation of the epithelium and innate immune cell infiltration of the LP (Fig. 3). We hypothesized that this could be a result of an altered inner mucus layer in the intestine, allowing for a closer microbe-epithelium interaction in metronidazole-treated mice than in untreated mice. To verify this, we assessed goblet cell function by transcriptional analysis of the goblet cell-specific proteins Muc2, intestinal trefoil factor (TFF3), and resistin-like molecule β (Relmβ). These proteins have defined roles in intestinal homeostasis: Muc2 is the main component of the intestinal mucin layer (26); intestinal trefoil factor (TFF3) synergizes with Muc2, enhancing the protective properties of the mucus layer (55); and Relmβ has an important role in innate immunity and host defense (3, 39). The results in Fig. 4A show that metronidazole treatment caused a significant downregulation of *Muc2*, *TFF3*, and *Relm*β mRNA expression in the distal colon, compared to that in untreated mice, strongly suggesting that goblet cell function was affected by metronidazole treatment. In contrast, streptomycin treatment did not affect the levels of *Muc2* and *TFF3* expression compared to those in untreated mice (Fig. 4A). The reduction in *Muc2* mRNA expression after metronidazole treatment was reflected by a significant decrease in the colonic inner mucus layer thickness, as shown by AB/PAS staining (Fig. 4B and C). While the inner mucus layer of untreated mice was on average 23 μm (±3 μm) thick (Fig. 4B), metronidazole-treated mice exhibited a significantly thinner inner mucus layer, measured to be 13 μm (±1 μm) thick, a reduction of 39% from that of untreated mice (Fig. 4B and C). The inner mucus layer of streptomycin-treated mice was on average 21 μm (±1 μm) thick and did not differ from that of untreated mice (Fig. 4B and C), corresponding to the unaltered *Muc2* mRNA expression in these animals. Thinning of the inner mucus layer in the distal colon induced by metronidazole treatment was confirmed by immunofluorescence using an antibody specific for murine Muc2 (Fig. 4D). These findings indicate that metronidazole treatment affects goblet cell Muc2 production, resulting in thinning of the inner mucus layer.

Metronidazole pretreatment increases the rate of *C. rodentium* attachment to IECs. *C. rodentium*-induced colitis 6 days p.i. was more severe in metronidazole-pretreated mice, but no difference in *C. rodentium* burden was seen (Fig. 1C and F). Moreover, metronidazole-treated animals showed evidence of increased inflammatory tone of the intestine characterized by increased bacterial stimulation of the epithelium (Fig. 3) and a thinner inner mucus layer (Fig. 4), suggesting a weakened mucosal barrier. To verify this, we performed immunostaining for the *C. rodentium*-derived infection marker Tir (translocated intimin receptor) on colon sections 2, 4, and 6 days p.i., as a measure of the rate of *C. rodentium* attachment to the intestinal epithelium. The results shown in Fig. 5 demonstrate that metronidazole pretreatment facilitates *C. rodentium* attachment to the epithelium (Fig. 5A), resulting in significantly higher numbers of colonic bacteria at the early stages of infection (Fig. 5B) and deeper penetration of *C. rodentium* earlier in infection, at 4 days p.i. (Fig. 5A, asterisk). At 21 days p.i., *C. rodentium* numbers in the colon decrease; however, a small subpopulation of metronidazole-pretreated mice remain highly colonized (Fig. 5B). Complementing the increase in *C.*

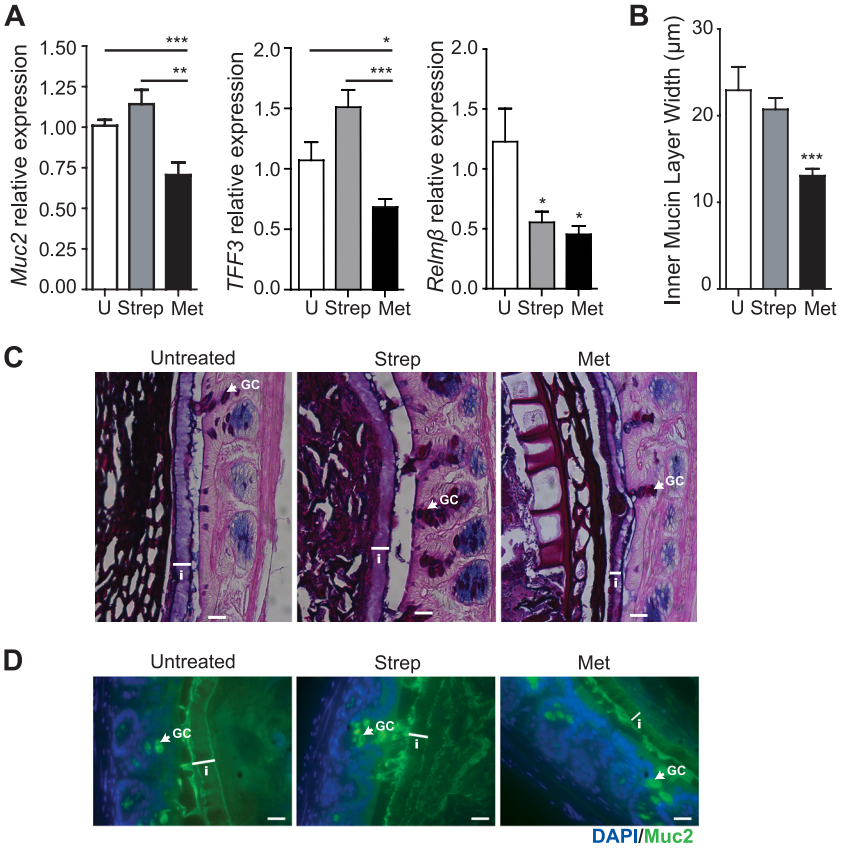

FIG. 4. Metronidazole treatment alters goblet cell function and reduces the production of the inner mucus layer. (A) Quantitative RT-PCR results of *Muc2*, *TFF3*, and *Relm*β expression in the distal colon. Results are averaged from three independent experiments ($n = 3$ to 6 mice per group). U, untreated mice; for *Muc2*, ***, $P = 0.0008$, and **, $P = 0.0017$; for *TFF3*, ***, $P < 0.0001$, and *, $P = 0.02$; for *Relm*β, Strep *, $P = 0.03$, and Met *, $P = 0.01$. (B) Quantification of inner mucin layer thickness. Distal colon sections were fixed in methanol-Carnoy's fixative, embedded in paraffin, and stained with AB/PAS to visualize and quantify the inner mucus layer. The inner mucus width was determined by an average of 4 measurements per field with 4 fields counted per tissue section. Results are averaged from two independent experiments ($n = 3$ mice per group). U, untreated mice; ***, $P = 0.0003$. (C) AB/PAS-stained methanol-Carnoy's fixative-fixed distal colon sections showing the inner mucin layer (white arrowheads). i, inner mucin layer; GC, goblet cell. Original magnification, ×400. Bars, 20 μm. (D) Representative immunostaining for the inner mucin layer using an antibody that recognizes murine Muc2 (green) with DAPI (blue) as a counterstain. The inner mucin layer is thinner in metronidazole-treated C57BL/6 mice. i, inner mucin layer; GC, goblet cell. Original magnification, ×400. Bars, 20 μm.

rodentium attachment to the epithelium, the production of proinflammatory cytokines upon *C. rodentium* infection also indicates differences in the inflammatory tone between untreated and metronidazole-treated mice (Fig. 5C). Colonic levels of tumor necrosis factor alpha (TNF-α), gamma interferon (IFN-γ), and monocyte chemoattractant protein 1 (MCP-1) were found to be 6-fold, 5-fold, and 4-fold higher, respectively, in metronidazole-pretreated, infected mice 2 days p.i. However, the expression of TNF-α, IFN-γ, and MCP-1 was not significantly higher prior to infection (data not shown) or at later days after infection in metronidazole-pretreated mice (Fig. 5C). Collectively, these results indicate that metronidazole treatment triggers an immune homeostatic imbalance in the intestinal epithelium, which might have an important impact on the severity of subsequent infections.

DISCUSSION

In this study, we have shown that metronidazole, but not streptomycin, pretreatment results in increased severity of *C. rodentium*-induced colitis. Further, we confirmed that the two antibiotics differentially alter the composition of the microbiota. Additionally, only metronidazole treatment resulted in altered goblet cell function and thinning of the inner mucus layer, resulting in microbially induced immune activation prior to disease induction.

The intestinal mucus layer plays a key role in the maintenance of intestinal homeostasis: it protects the epithelium from dehydration, physical abrasion, and invading microorganisms (33). Muc2-deficient mice, which have an altered intestinal mucus layer, are more susceptible to the development and perpetuation of dextran sulfate sodium (DSS)- and *C. rodentium*-induced colitis (6, 54, 55) due to a closer interaction of intestinal microbes with the epithelial barrier. Recent work has also shown that most of the antimicrobial activity of the intestinal lumen localizes to the mucin layer (27), attesting to its role as a barrier to bacterial penetration of the epithelium. The thickness of the inner mucus layer varies along the length of the intestinal tract and is thickest in the most distal portion (4), which also harbors the highest concentrations of bacteria. We

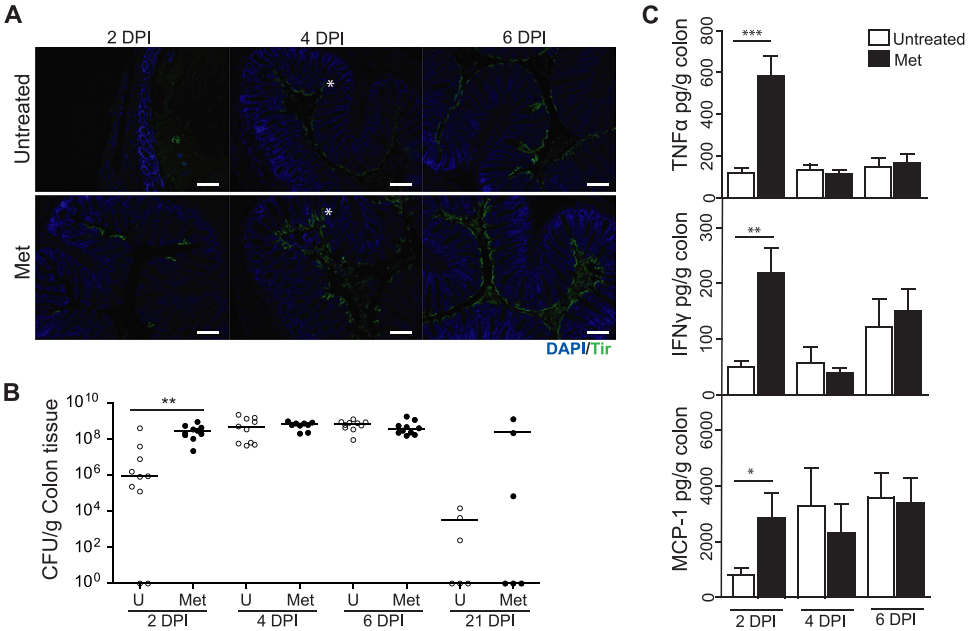

FIG. 5. Metronidazole pretreatment increases the rate of *C. rodentium* attachment to intestinal epithelial cells. (A) Representative immunostaining for the *C. rodentium*-specific effector Tir (green) in colon, with DAPI (blue) as a counterstain, at various time points for untreated and metronidazole-pretreated mice. Note Tir staining present at day 2 p.i. in metronidazole-pretreated mice, which is absent in untreated mice. *C. rodentium* penetrates deeper into crypts of metronidazole-pretreated mice than it does into those of untreated mice on day 4 p.i. (asterisk). Original magnification, ×100. Bars, 100 μm. (B) Enumeration of *C. rodentium* bacteria in the colon at days 2, 4, 6, and 21 p.i. (2 DPI, 4 DPI, 6 DPI, and 21 DPI, respectively). Each data point represents one individual. Results are pooled from two separate infections ($n = 4$ to 6 per group). **, $P = 0.0068$. Day 21 p.i. results represent a single experiment ($n = 6$). The horizontal lines represent the median for each group. U, untreated. (C) Cytokine and chemokine production in the colon at days 2, 4, and 6 p.i. (2 DPI, 4 DPI, and 6 DPI, respectively). Results are pooled from two separate infections ($n = 4$ to 6 per group). Cytokines TNF-α and IFN-γ and chemokine MCP-1 are produced at 6-fold (***, $P = 0.0007$)-, 5-fold (**, $P = 0.0033$)-, and 4-fold (*, $P = 0.0343$)-higher levels, respectively, at day 2 p.i. in metronidazole-pretreated mice than in untreated mice.

have shown here that metronidazole-induced changes in the microbiota composition associate with a decrease in Muc2 production and reduction of the inner mucus layer in the distal colon. The metronidazole-induced reduction in the *Bacteroidales* order within the *Bacteroidetes* phylum is particularly interesting; members of the *Bacteroidetes* phylum, specifically *Bacteroides thetaiotaomicron*, have been shown to be important colonizers and grazers of the outer mucus layer in humans (29, 37, 49). Degradation of these mucin peptides and O-linked glycans serves as an energy source for the intestinal microbiota and consequently results in the production of short-chain fatty acids such as acetate and butyrate (15, 25), which are able to diffuse through the inner mucus layer and stimulate the underlying epithelial cells to produce Muc2 (10, 11). The mechanism by which metronidazole treatment causes a reduction in the expression of *Muc2* may be the breaking up of an important feedback mechanism between commensal utilization of mucins and host production of mucins. A recent study has shown that metronidazole treatment results in thickening of the mucus layer in the proximal colon of rats (41). The reasons for this discrepancy with our results may be due to the different dose of metronidazole administered and area of intestinal tract studied. Additionally, although this study suggests that metronidazole causes thickening of the mucus layer, it has also shown a closer association of microbes with the intestinal epithelium (41). This closer microbe-IEC interaction would be more consistent with our findings that metronidazole causes thinning of the inner mucus layer, which acts as a barrier between the microbiota and epithelium, which is devoid of bacteria (26). The authors also speculated that a thickened mucus layer was associated with increased *Bifidobacterium* spp.; however, this population of bacteria was undetectable in all treatment groups in our study.

Metronidazole treatment did not cause any overt signs of inflammation in the distal colon; however, we did note an increase in the expression of both *IL-25* and *Reg3*γ mRNA with no effect on other cytokines secreted by intestinal epithelial cells, such as *TSLP*. In light of previous studies (9, 12, 28, 59), this is interpreted as increased stimulation of the colonic epithelium by the microbiota as a result of a depleted inner mucus layer. This increase in epithelial stimulation was accompanied by recruitment of NK cells and macrophages to the lamina propria, suggesting the development of a proinflammatory immunological tone. Our findings are consistent with similar experiments performed in Muc2-knockout mice, showing that these mice exhibit enhanced mucosal permeability and subclinical levels of chronic inflammation due to increased stimulation of epithelial cells by intestinal bacteria (55, 58). *C. rodentium* infection of metronidazole-pretreated animals resulted in robust TNF-α and IFN-γ cytokine and MCP-1 chemokine production early in infection, a finding which further strengthens the interpretation that metronidazole treatment triggers an immune homeostatic imbalance. Upon infection by *C. rodentium*, innate immune cells, including epithelial cells, NK cells, and macrophages, respond by production of TNF-α, IFN-γ, and MCP-1. If these cells are already stimu-

lated and recruited prior to infection, the initial inflammatory response would be heightened, as is observed in metronidazole-pretreated mice.

In keeping with the recognized roles of the mucus layer, the reduction of its thickness may have allowed for increased attachment of *C. rodentium* to the intestinal epithelium. This fact most likely represents a major factor contributing to the exacerbated severity of *C. rodentium*-induced colitis in metronidazole-pretreated animals. It has been previously shown that colonizing the outer and inner mucus layer is a key step for the pathogenesis of *C. rodentium* and other attaching and effacing pathogens (5). However, we cannot eliminate the possibility that the increased *C. rodentium* attachment results from the elimination of intestinal bacteria that are natural competitors of *C. rodentium*. Metronidazole treatment resulted in the most drastic change in microbiota composition. However, if the compositional changes result in a competitive advantage and/or newly vacant niches for *C. rodentium*, we would have expected to detect an increase in *C. rodentium* burden, but this was not the case. In fact, *C. rodentium* colonization of the cecum, colon, and mesenteric lymph nodes of metronidazole-pretreated mice was equivalent to that of untreated mice at 6 days p.i.

Our results have serious implications with regard to the use of antibiotics in the treatment of chronic intestinal inflammatory conditions such as IBD. Metronidazole is used extensively in the treatment of IBD, with variable efficacy (20, 45). In ulcerative colitis, metronidazole has been found to be ineffective in double-blind, placebo-controlled trials, compared to standard steroid treatment (13, 36). In Crohn's disease, the use of metronidazole is still highly controversial, as it shows variable efficacy (2, 8, 51, 52). Streptomycin treatment did not show the same effects as did metronidazole; thus, our data outline a scenario in which certain antibiotic treatments (e.g., metronidazole) would have an effect on both the microbial composition and the immune status of the intestine. We show that metronidazole treatment has a dramatic impact on the immunological tone of the intestinal epithelium, altering goblet cell function and thus leading to thinning of the inner mucus layer, changes that are punctuated by an increased susceptibility to enteric pathogens. Such a chain of events may very well contribute to the onset or maintenance of chronic intestinal inflammatory conditions and promote the occurrence of opportunistic enteric infections.

The difference in outcomes between the streptomycin and metronidazole treatments strongly suggests that the antibiotic effects on the intestinal environment are driven by their distinct impact on the intestinal commensal population. Future studies aim to elucidate the mechanism by which the microbiota may control or influence goblet cell function and mucus production in the intestine. We have shown that a specific shift in the microbiota composition results in intestinal homeostatic imbalance and diminished expression of Muc2 and thinning of the inner mucus layer, leading to increased susceptibility to *C. rodentium*-induced colitis.

ACKNOWLEDGMENTS

We thank members of the Finlay lab for helpful insights and suggestions, specifically M. A. Croxen for helpful edits and discussions of the manuscript.

M.W. is a Michael Smith Foundation for Health Research (MSFHR) and Crohn's and Colitis Foundation of Canada (CCFC) Junior Graduate Trainee. B.B.F. is a Howard Hughes International Research Scholar, a CIHR Distinguished Investigator, and the UBC Peter Wall Distinguished Professor. This study was funded through operating grants from the Canadian Institute for Health Research and the CCFC.

REFERENCES

1. **Amann, R. I., et al.** 1990. Combination of 16S rRNA-targeted oligonucleotide probes with flow cytometry for analyzing mixed microbial populations. Appl. Environ. Microbiol. **56:**1919–1925.
2. **Ambrose, N. S., et al.** 1985. Antibiotic therapy for treatment in relapse of intestinal Crohn's disease. A prospective randomized study. Dis. Colon Rectum **28:**81–85.
3. **Artis, D., et al.** 2004. RELMbeta/FIZZ2 is a goblet cell-specific immune-effector molecule in the gastrointestinal tract. Proc. Natl. Acad. Sci. U. S. A. **101:**13596–13600.
4. **Atuma, C., V. Strugala, A. Allen, and L. Holm.** 2001. The adherent gastrointestinal mucus gel layer: thickness and physical state in vivo. Am. J. Physiol. Gastrointest. Liver Physiol. **280:**G922–G929.
5. **Bergstrom, K. S., et al.** 2008. Modulation of intestinal goblet cell function during infection by an attaching and effacing bacterial pathogen. Infect. Immun. **76:**796–811.
6. **Bergstrom, K. S., et al.** 2010. Muc2 protects against lethal infectious colitis by disassociating pathogenic and commensal bacteria from the colonic mucosa. PLoS Pathog. **6:**e1000902.
7. **Biswas, D. K., and L. Gorini.** 1972. The attachment site of streptomycin to the 30S ribosomal subunit. Proc. Natl. Acad. Sci. U. S. A. **69:**2141–2144.
8. **Blichfeldt, P., J. P. Blomhoff, E. Myhre, and E. Gjone.** 1978. Metronidazole in Crohn's disease. A double blind cross-over clinical trial. Scand. J. Gastroenterol. **13:**123–127.
9. **Brandl, K., et al.** 2008. Vancomycin-resistant enterococci exploit antibiotic-induced innate immune deficits. Nature **455:**804–807.
10. **Brown, A. J., et al.** 2003. The orphan G protein-coupled receptors GPR41 and GPR43 are activated by propionate and other short chain carboxylic acids. J. Biol. Chem. **278:**11312–11319.
11. **Burger-van Paassen, N., et al.** 2009. The regulation of intestinal mucin MUC2 expression by short-chain fatty acids: implications for epithelial protection. Biochem. J. **420:**211–219.
12. **Cash, H. L., C. V. Whitham, C. L. Behrendt, and L. V. Hooper.** 2006. Symbiotic bacteria direct expression of an intestinal bactericidal lectin. Science **313:**1126–1130.
13. **Chapman, R. W., W. S. Selby, and D. P. Jewell.** 1986. Controlled trial of intravenous metronidazole as an adjunct to corticosteroids in severe ulcerative colitis. Gut **27:**1210–1212.
14. **Deng, W., B. A. Vallance, Y. Li, J. L. Puente, and B. B. Finlay.** 2003. Citrobacter rodentium translocated intimin receptor (Tir) is an essential virulence factor needed for actin condensation, intestinal colonization and colonic hyperplasia in mice. Mol. Microbiol. **48:**95–115.
15. **Dharmani, P., V. Srivastava, V. Kissoon-Singh, and K. Chadee.** 2009. Role of intestinal mucins in innate host defense mechanisms against pathogens. J. Innate Immun. **1:**123–135.
16. **Dore, J., A. Sghir, G. Hannequart-Gramet, G. Corthier, and P. Pochart.** 1998. Design and evaluation of a 16S rRNA-targeted oligonucleotide probe for specific detection and quantitation of human faecal Bacteroides populations. Syst. Appl. Microbiol. **21:**65–71.
17. **Frank, D. N., et al.** 2007. Molecular-phylogenetic characterization of microbial community imbalances in human inflammatory bowel diseases. Proc. Natl. Acad. Sci. U. S. A. **104:**13780–13785.
18. **Franks, A. H., et al.** 1998. Variations of bacterial populations in human feces measured by fluorescent in situ hybridization with group-specific 16S rRNA-targeted oligonucleotide probes. Appl. Environ. Microbiol. **64:**3336–3345.
19. **Garrett, W. S., et al.** 2007. Communicable ulcerative colitis induced by T-bet deficiency in the innate immune system. Cell **131:**33–45.
20. **Gionchetti, P., et al.** 2006. Antibiotics and probiotics in treatment of inflammatory bowel disease. World J. Gastroenterol. **12:**3306–3313.
21. **Hoebler, C., E. Gaudier, P. De Coppet, M. Rival, and C. Cherbut.** 2006. MUC genes are differently expressed during onset and maintenance of inflammation in dextran sodium sulfate-treated mice. Dig. Dis. Sci. **51:**381–389.
22. **Hollingsworth, M. A., and B. J. Swanson.** 2004. Mucins in cancer: protection and control of the cell surface. Nat. Rev. Cancer **4:**45–60.
23. **Hooper, L. V.** 2009. Do symbiotic bacteria subvert host immunity? Nat. Rev. Microbiol. **7:**367–374.
24. **Ivanov, I. I., et al.** 2008. Specific microbiota direct the differentiation of IL-17-producing T-helper cells in the mucosa of the small intestine. Cell Host Microbe **4:**337–349.
25. **Johansson, M. E., J. M. Holmen Larsson, and G. C. Hansson.** 25 June 2010, posting date. Microbes and Health Sackler Colloquium: the two mucus layers of colon are organized by the MUC2 mucin, whereas the outer layer

is a legislator of host-microbial interactions. Proc. Natl. Acad. Sci. U. S. A. doi:10.1073/pnas.1006451107.
26. **Johansson, M. E., et al.** 2008. The inner of the two Muc2 mucin-dependent mucus layers in colon is devoid of bacteria. Proc. Natl. Acad. Sci. U. S. A. **105:**15064–15069.
27. **Johansson, M. E., K. A. Thomsson, and G. C. Hansson.** 2009. Proteomic analyses of the two mucus layers of the colon barrier reveal that their main component, the Muc2 mucin, is strongly bound to the Fcgbp protein. J. Proteome Res. **8:**3549–3557.
28. **Keilbaugh, S. A., et al.** 2005. Activation of RegIIIbeta/gamma and interferon gamma expression in the intestinal tract of SCID mice: an innate response to bacterial colonisation of the gut. Gut **54:**623–629.
29. **Kline, K. A., S. Falker, S. Dahlberg, S. Normark, and B. Henriques-Normark.** 2009. Bacterial adhesins in host-microbe interactions. Cell Host Microbe **5:**580–592.
30. **Langendijk, P. S., et al.** 1995. Quantitative fluorescence in situ hybridization of Bifidobacterium spp. with genus-specific 16S rRNA-targeted probes and its application in fecal samples. Appl. Environ. Microbiol. **61:**3069–3075.
31. **Legendre, P., and L. Legendre.** 1998. Numerical ecology, 2nd English ed., vol. 2. Elsevier, Amsterdam, Netherlands.
32. **Lepage, P., et al.** 2005. Biodiversity of the mucosa-associated microbiota is stable along the distal digestive tract in healthy individuals and patients with IBD. Inflamm. Bowel Dis. **11:**473–480.
33. **Linden, S. K., P. Sutton, N. G. Karlsson, V. Korolik, and M. A. McGuckin.** 2008. Mucins in the mucosal barrier to infection. Mucosal Immunol. **1:**183–197.
34. **Mack, D. R., S. Michail, S. Wei, L. McDougall, and M. A. Hollingsworth.** 1999. Probiotics inhibit enteropathogenic E. coli adherence in vitro by inducing intestinal mucin gene expression. Am. J. Physiol. **276:**G941–G950.
35. **Makkink, M. K., et al.** 2002. Fate of goblet cells in experimental colitis. Dig. Dis. Sci. **47:**2286–2297.
36. **Mantzaris, G. J., A. Hatzis, P. Kontogiannis, and G. Triadaphyllou.** 1994. Intravenous tobramycin and metronidazole as an adjunct to corticosteroids in acute, severe ulcerative colitis. Am. J. Gastroenterol. **89:**43–46.
37. **Martens, E. C., R. Roth, J. E. Heuser, and J. I. Gordon.** 2009. Coordinate regulation of glycan degradation and polysaccharide capsule biosynthesis by a prominent human gut symbiont. J. Biol. Chem. **284:**18445–18457.
38. **Mundy, R., T. T. MacDonald, G. Dougan, G. Frankel, and S. Wiles.** 2005. Citrobacter rodentium of mice and man. Cell. Microbiol. **7:**1697–1706.
39. **Nair, M. G., et al.** 2008. Goblet cell-derived resistin-like molecule beta augments CD4+ T cell production of IFN-gamma and infection-induced intestinal inflammation. J. Immunol. **181:**4709–4715.
40. **Pedron, T., and P. Sansonetti.** 2008. Commensals, bacterial pathogens and intestinal inflammation: an intriguing menage a trois. Cell Host Microbe **3:**344–347.
41. **Pelissier, M. A., et al.** 2010. Metronidazole effects on microbiota and mucus layer thickness in the rat gut. FEMS Microbiol. Ecol. **73:**601–610.
42. **Rinttila, T., A. Kassinen, E. Malinen, L. Krogius, and A. Palva.** 2004. Development of an extensive set of 16S rDNA-targeted primers for quantification of pathogenic and indigenous bacteria in faecal samples by real-time PCR. J. Appl. Microbiol. **97:**1166–1177.
43. **Round, J. L., and S. K. Mazmanian.** 2009. The gut microbiota shapes intestinal immune responses during health and disease. Nat. Rev. Immunol. **9:**313–323.
44. **Salzman, N. H., M. A. Underwood, and C. L. Bevins.** 2007. Paneth cells, defensins, and the commensal microbiota: a hypothesis on intimate interplay at the intestinal mucosa. Semin. Immunol. **19:**70–83.
45. **Sartor, R. B.** 2004. Therapeutic manipulation of the enteric microflora in inflammatory bowel diseases: antibiotics, probiotics, and prebiotics. Gastroenterology **126:**1620–1633.
46. **Scanlan, P. D., et al.** 2008. Culture-independent analysis of the gut microbiota in colorectal cancer and polyposis. Environ. Microbiol. **10:**789–798.
47. **Searle, A. J., and R. L. Willson.** 1976. Metronidazole (Flagyl): degradation by the intestinal flora. Xenobiotica **6:**457–464.
48. **Sekirov, I., et al.** 2008. Antibiotic-induced perturbations of the intestinal microbiota alter host susceptibility to enteric infection. Infect. Immun. **76:**4726–4736.
49. **Sonnenburg, J. L., L. T. Angenent, and J. I. Gordon.** 2004. Getting a grip on things: how do communities of bacterial symbionts become established in our intestine? Nat. Immunol. **5:**569–573.
50. **Stecher, B., and W. D. Hardt.** 2008. The role of microbiota in infectious disease. Trends Microbiol. **16:**107–114.
51. **Sutherland, L., et al.** 1991. Double blind, placebo controlled trial of metronidazole in Crohn's disease. Gut **32:**1071–1075.
52. **Thia, K. T., et al.** 2009. Ciprofloxacin or metronidazole for the treatment of perianal fistulas in patients with Crohn's disease: a randomized, double-blind, placebo-controlled pilot study. Inflamm. Bowel Dis. **15:**17–24.
53. **Thim, L.** 1997. Trefoil peptides: from structure to function. Cell. Mol. Life Sci. **53:**888–903.
54. **van der Sluis, M., et al.** 2008. Combined defects in epithelial and immunoregulatory factors exacerbate the pathogenesis of inflammation: mucin 2-interleukin 10-deficient mice. Lab. Invest. **88:**634–642.
55. **Van der Sluis, M., et al.** 2006. Muc2-deficient mice spontaneously develop colitis, indicating that MUC2 is critical for colonic protection. Gastroenterology **131:**117–129.
56. **Van Klinken, B. J., J. Dekker, H. A. Buller, and A. W. Einerhand.** 1995. Mucin gene structure and expression: protection vs. adhesion. Am. J. Physiol. **269:**G613–G627.
57. **Willing, B., et al.** 2009. Changes in faecal bacteria associated with concentrate and forage-only diets fed to horses in training. Equine Vet. J. **41:**908–914.
58. **Yang, K., et al.** 2008. Interaction of Muc2 and Apc on Wnt signaling and in intestinal tumorigenesis: potential role of chronic inflammation. Cancer Res. **68:**7313–7322.
59. **Zaph, C., et al.** 2008. Commensal-dependent expression of IL-25 regulates the IL-23-IL-17 axis in the intestine. J. Exp. Med. **205:**2191–2198.

Editor: A. J. Bäumler